FOI
SWEDISH DEFENCE
RESEARCH AGENCY

FOI-R—0591—SE
September 2002
ISSN 1650-1942
Technical report

Anders Larsson

The voltage gradient along a lightning channel during strikes to aircraft

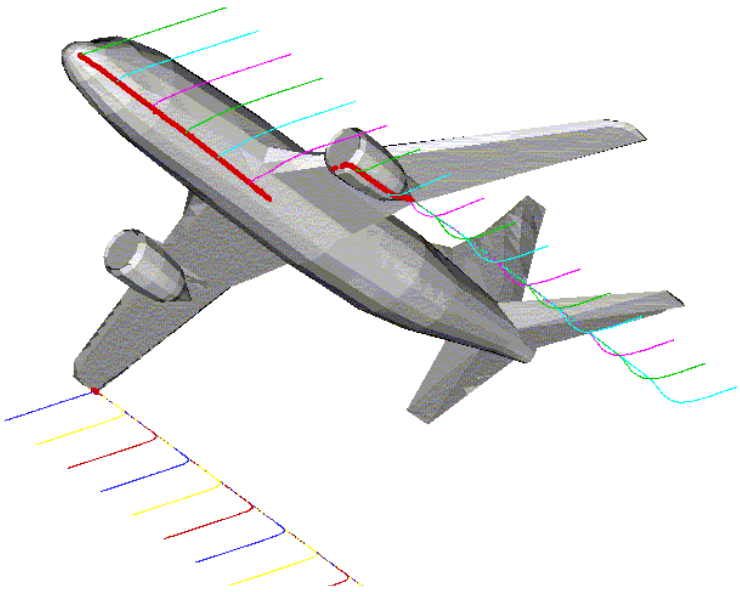

Weapons and Protection
SE-147 25 Tumba

SWEDISH DEFENCE RESEARCH AGENCY
Weapons and Protection
SE-147 25 TUMBA

FOI-R— 0591—SE
September 2002
ISSN 1650-1942
Technical report

Anders Larsson

The voltage gradient along a lightning channel during strikes to aircraft

Issuing organization	Report number, ISRN	Report type
FOI – Swedish Defence Research Agency Weapons and Protection SE-147 25 TUMBA	FOI-R—0591—SE	Technical report
	Research area code 6. Electronic Warfare	
	Month year September 2002	**Project no.** E2222
	Customers code 5. Contracted Research	
	Sub area code 61 Electronic Warfare, Electromagnetic Weapons	

Author/s (editor/s)	Project manager
Anders Larsson	Anders Larsson
	Approved by Torgny Carlsson
	Sponsoring agency
	Scientifically and technically responsible

Report title

The voltage gradient along a lightning channel during strikes to aircraft

Abstract (not more than 200 words)

Lightning strike to aircraft is a threat to flight safety. During the strike, the lightning channel sweeps along the body of the aircraft. The voltage gradient of the lightning channel is one important property that determines where on the aircraft it may sweep is its voltage gradient. This report presents an analysis of this voltage gradient for the purpose of numerical lightning swept stroke simulations.

Keywords

Lightning, aircraft, numerical simulation

Further bibliographic information	Language English
ISSN 1650-1942	**Pages:** 15 pages
	Price acc. to pricelist

Utgivare FOI – Totalförsvarets Forskningsinstitut Vapen och skydd 147 25 TUMBA	**Rapportnummer, ISRN** FOI-R—0591—SE	**Klassificering** Teknisk rapport
	Forskningsområde 6. Telekrig	
	Månad, år September 2002	**Projektnummer** E2222
	Verksamhetsgren 5. Uppdragsfinansierad verksamhet	
	Delområde 61 Telekrigföring med EM-vapen och skydd	
Författare/redaktör Anders Larsson	**Projektledare** Anders Larsson	
	Godkänd av Torgny Carlsson	
	Uppdragsgivare/kundbeteckning	
	Tekniskt och/eller vetenskapligt ansvarig	

Rapportens titel (i översättning)

Spänningsfallet längs en blixtkanal vid nedslag i flygplan

Sammanfattning (högst 200 ord)

Blixtnedslag i flygplan är ett hot mot flygsäkerheten. När ett flygplan träffas av blixten sveper blixtkanalen längs flygplanskroppen. En viktig egenskap hos blixtkanalen som bestämmer var på flygplanskroppen som den kan befinna sig är spänningsfallet längs kanalen. I denna rapport analyseras detta spänningsfall för att användas i numeriska beräkningar av hur blixtkanalen sveper längs en flygplanskropp.

Nyckelord

Blixtnedslag, flygplan, numeriska simuleringar

Övriga bibliografiska uppgifter	**Språk** Engelska
ISSN 1650-1942	**Antal sidor:** 15 sidor
Distribution enligt missiv	**Pris: Enligt prislista**

Contents

1. Executive summary

This is the final report regarding Onera Order No 23215/DA/BHUG. This project lasted from October 2001 to Septemer 2002 with Dr Anders Larsson, Swedish Defence Research Agency, as the contractor with a project budget of 7622,45 EUR (50 kFRF) and is a continuation of previous collaboration [1,2,3]. One project meeting has been held: 10–11 June 2002 in Paris, France. This project was also discussed during the Onera workshop on The Physics of Thundercloud and Lightning Discharges, Châtillon (Paris), France, November 2001. The results of this project will be submitted to the 12th *International Conference on Atmospheric Electricity*, 9-13 June 2003, Versailles, France [4]. Furthermore, these results are in part included in the invited paper to *Comptes Rendus Physiqu*e by Dr Larsson [5].

2. Introduction

In the design of aircraft it is important to determine the locations of where the lightning can have its initial attachment points on the aircraft and over which areas the attachment point may sweep. The determination of these locations and areas are called *aircraft zoning* and a generic way of performing this zoning is shown in Figure 1, where a roadmap towards a simulation tool to determine the lightning swept stroke zones is sketched [5]. As shown in the figure, two physical processes must be modelled: the inception of the lightning flash and the sweeping of the lightning channel along the aircraft.

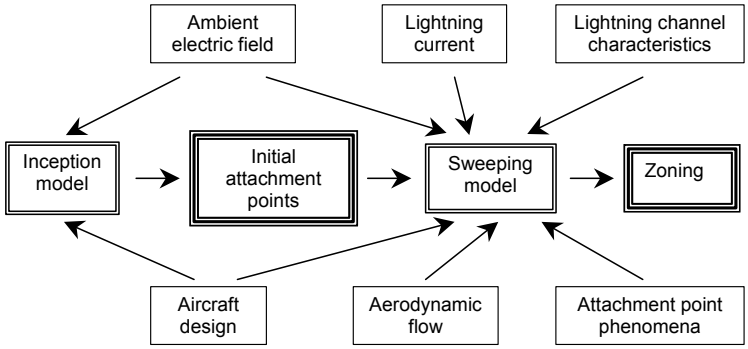

Figure 1. *A roadmap towards a design tool to determine the initial attachment points and the swept stroke zones [5]. The core of the roadmap is the two models of the lightning inception and lightning sweeping and their dependencies.*

The points from where a stable-propagating lightning leader discharge can be initiated determine the locations of the initial attachment points. The initial attachment of a lightning channel occurs within a few milliseconds and is thus so rapid process that the sweeping phenomena can be neglected. The parameters that govern the location of the initial attachment points are the aircraft geometry and the ambient electric field. The sweeping phase is more complex than the initial attachment phase, mainly because its longer duration (up to one second) which implies that considering typical aircraft speeds the lightning channel can be displaced along the whole aircraft during the existence of the lightning flash. As for the initial attachment, the aircraft design and the electric field environment are important factors, but also the interaction between the lightning current, the lightning channel characteristics and the aerodynamic flow must be considered.

The lightning channel may reattach downstream the attachment point or to other parts of the aircraft and at that location form a new attachment point. Reattachment occurs when the potential drop along the channel together with the channel displacement and deformation due to the aerodynamic flow create a situation where there is a favourable condition for an electrical breakdown between a segment of the channel and the surface. Thus, the voltage gradient along the lightning channel is a crucial property of the channel that determines possible reattachments. This report presents an analysis of this voltage gradient for the purpose of numerical lightning swept stroke simulations.

3. Voltage gradient

The internal electric field strength of, or voltage gradient along, the lightning channel is, as mentioned above, of central importance. This voltage gradient is the cause of the voltage build-up along the lightning channel that is required for possible reattachment. The voltage gradient, E, is given by the lightning current and channel properties according to

$$E = E_{\text{res}} + E_{\text{ind}} = R(I,t) \cdot I(t) + L\frac{\partial I(t)}{\partial t} \qquad (1)$$

where $I(t)$ is the lightning current, R is resistance per unit length of the channel and L is the inductance per unit length. The subdivision of the voltage gradient into a resistive part E_{res} and an inductive one E_{ind} is enlightening.

4. Lightning current

The understanding of the lightning strike to aircraft has been greatly enhanced during the last years thanks to a comprehensive analysis of available in-flight data [6]. A lightning stike to aircraft starts with the development of a positive discharge from the aircraft, followed by, a few milliseconds later, the inception of a negative discharge propagating in the opposite direction; a bi-directional leader. During the lightning flash, the aircraft forms a part of the lightning current path. The lightning current consists of a continuing current of about 300 A with a duration of about 200 ms, with superimposed high-amplitude currents (recoil leaders [7]). The data for the current impulses from the in-flight campaigns are uncertain because of poor sampling rate and other measurement problems. However, the measured peak current was up to 20 kA and its time derivative up to 10^{10} A/s = 10 kA/μs. Furthermore, when the continuing current eventually has vanished, current impulses still may occur. For a typical waveform of the lightning current, see Figure 2.

For numerical simulation of lightning swept strokes, it would be most beneficial to have some kind of analytical expressions for the different phases of the lightning current. The shape of the lightning current during the continuing current phase is trivial. However, the shape of the current during the current impulses (return strokes and recoil leaders) must be carefully considered, especially since its time derivative is required in the expression of the inductive part of the voltage gradient of the lightning channel. In the search for an analytical expression for the time-dependence of the current, $I(t)$, appropriate for simulations, the conventional double-exponential function for impulses will not be appropriate here since it gives an infinite derivative of the current at the beginning of the impulse. The IEC function of the lightning current for analysis purposes overcome this problem [8]:

$$I(t) = \frac{I_{\max}}{h} \frac{(t/\tau_1)^{10}}{1+(t/\tau_1)^{10}} \exp\left(-\frac{t}{\tau_2}\right) \qquad (2)$$

where I_{max} is the peak current and h is a correction factor for the peak current, τ_1 and τ_2 are the time constants for the front time and tail time, respectively. The IEC document stipulates the current waveform 10/350 μs (h = 0,93, τ_1 = 19 μs, τ_2 = 485 μs) for the first return stroke and waveform 0,15/100 μs (h = 0,993, τ_1 = 0,454 μs, τ_2 = 143 μs) for subsequent strokes. However, one should bear in mind that the IEC function regards the current at ground for cloud-to-ground lightning flashes. Measured data for the current amplitude and maximum time derivative of the current can be found in the literature [6,9]. For example, as mentioned in the introduction, in-flight measurements give peak currents up to 20 kA and peak time derivatives up to 10^{10} A/s. In a practical numerical simulation of the whole flash, the time step required to resolve the current impulses would imply a long computational time. Instead of simulate the detailed behaviour, one may assume that the impulse take place during only one time step with a given peak current and a given time derivative. Such an approach also eliminates any requirements of assumptions about the real shape of the current during return strokes and recoil leaders.

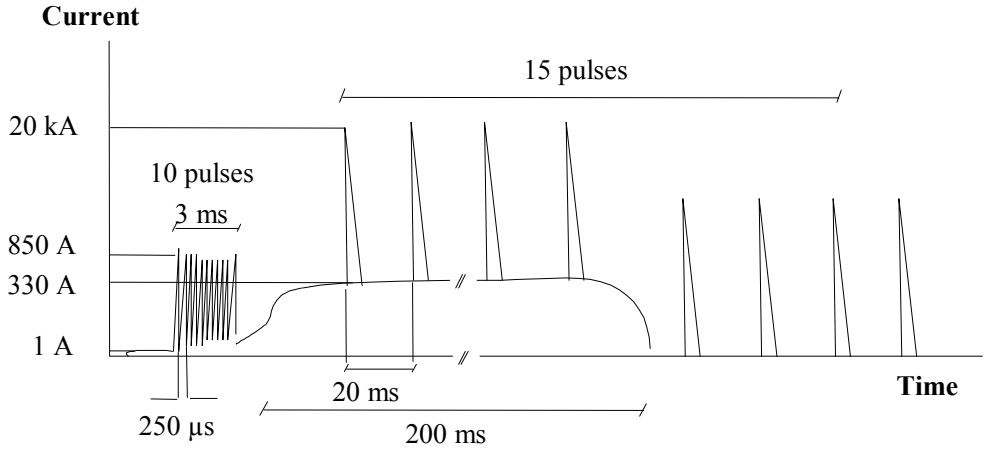

Figure 2. *Typical waveform of the discharge current during a lightning strike to an aircraft as inferred from in-flight measurements [6].*

5. Impulse current phase

The inductance per unit length of the lightning channel can be approximated by the one of an isolated conductor of radius r_c and of length $h >> r_c$ as given by [10]

$$L \approx \frac{\mu_0}{2\pi} \ln\left(\frac{h}{r_c}\right) = 0{,}2 \cdot \ln\left(\frac{h}{r_c}\right) \ \mu\text{H/m} \qquad (3)$$

which is plotted in Figure 3. As can be seen in the figure, the inductance per unit length is only weakly dependent on the channel radius and is roughly constant about 2,0 ± 0,5 μH/m. Thus, a constant value of 2 μH/m is an adequate approximation of the magnitude of the inductance per unit length of the lightning channel.

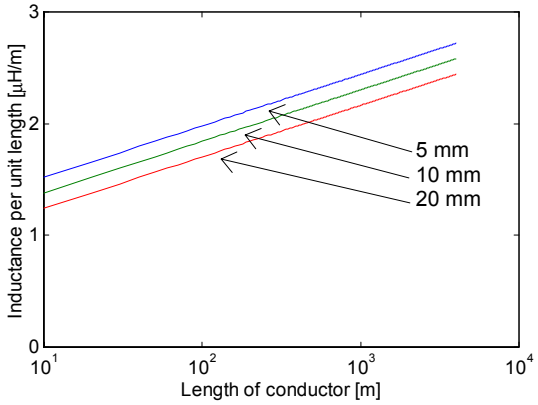

Figure 3. *The inductance per unit length of a single conductor according to equation (3) for three different values of the conductor radius (5 mm, 10 mm and 20 mm).*

Typical values for the resistance per unit length of a lightning channel during return stokes are in the range 0,01 – 0,1 Ω/m [10]. However, the resistance of the channel has a complex time and current dependence. The resistance will be further discussed in the next section.

Trivially, the resistive current will dominate the build-up of the voltage gradient during the continuing current phase. However, the situation is not that obvious during return strokes and recoil leaders. The contribution by the inductance can be estimated by

$$E_{\text{ind}} = L \cdot \frac{\partial I}{\partial t} \approx 2 \cdot 10^{-6} \times 10^{11} = 2 \cdot 10^{5}\ \text{V/m} \qquad (4)$$

and the contribution by the resistance

$$E_{\text{res}} = R \cdot I \approx 0{,}1 \times 20 \cdot 10^{3} = 2 \cdot 10^{3}\ \text{V/m} \qquad (5)$$

Thus, $E_{\text{ind}} >> E_{\text{res}}$ and the voltage gradient that is inductively built-up clearly dominate, and it is clear that very high values of the internal field are generated allowing longer jumps of the channel.

The decay of conductivity of the channel after the transient current phase of the return strokes and the recoil leaders has to be recognised, as well as the development of the resistance of the channel during the zero-current intervals. Gallimberti and Stangherlin [11] calculated the thermal decay of leader channel when no current flows through it. The initial temperature profile was assumed to have a Gaussian shape. For a temperature maximum of 5000 K and a Gaussian radius of 0,8 mm, the maximum temperature of the channel decays to a value below 1500 K in about 1,2 ms. The limiting value of 1500 K was chosen since below that temperature the electrons stay attached to oxygen molecules. A decay time constant of about 1 ms is consistent with the studies of Lowke et al [12]. Furthermore, Aleksandrov et al [13] have studied the channel decay for the situation when the current impulse is followed by a continuing current, where the channel decays to a steady-state situation after a duration of the order of 1 ms.

6. Continuing current phase

6.1 Long arc experimental data

A group of researchers at the Yokosuka Research Laboratory of the Central Research Institute of Electric Power Industry in Japan has studied the behaviour of long arcs for the application of faults in high-voltage transmission lines [14,15,16,17]. They studied both horizontal and vertical electrode arrangements. The electrodes consisted of different rod electrodes with a radius of 10 mm made of iron, copper or aluminium. The electrode distance was in the range 0,1 – 3,2 m and with an arc current in the range 0,05 – 10 kA. The arc was initiated by fusing a thin copper wire (radius 0,2 mm) that was initially short-circuiting the electrode gap. A general conclusion from their studies is that "free arcs, which have no restrictions such as a stabilising wall or forced external flow, show complex motion due to the effects of electromagnetic force and natural convection flow" [17].

They have measured the arc current and the voltage across the electrode gap. Furthermore, they have recorded the arc behaviour with either one high-speed video camera with a frame rate of 1000 frames per second or with two video cameras with a recording frame rate of 500 frames per second. From these measurements, they have estimated the true length of the tortuous path of the arc channel, the voltage gradient along the channel, the expansion radius of the erratic motion of the channel and finally the velocity of the channel during the erratic motion. See Figure 4 for an illustration of the expansion radius.

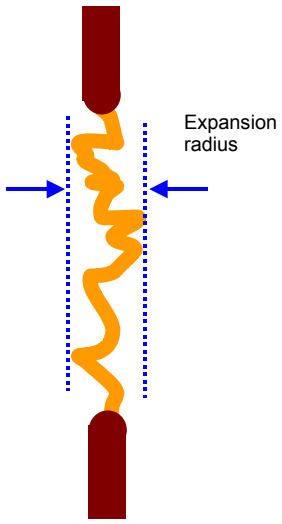

Figure 4. An arc discharge between two rod electrodes where the expansion radius is defined.

They present empirical interpolation formulas for the voltage gradient E, true (relative) length of arc channel L and the magnitude of the expansion radius R. Three magnitudes of the arc current (100 A, 500 A and 2000 A) with time duration of 100 ms were used. Three different gap distances were studied (1,6 m, 2,4 m, 3,2 m) but no influence of the gap distance was found.

Their interpolation formulae are given by

$$E = \alpha_E \cdot t^{-\beta_E} \tag{6}$$

$$L = 1 + \alpha_L \cdot t^{\beta_L} \quad (7)$$

$$R = \alpha_R \cdot t^{\beta_R} \quad (8)$$

where t is the time. The empirical coefficients α and β are found in Table 1. These formulas are plotted in Figures 5-7. Figure 2 gives that the voltage gradient converges towards values in the range 450 – 700 V/m with the lower values for the higher currents. It is interesting to compare the tortuosity factor here with the one achieved by the Les Renardières group in their long sparks experiments [18,19]. They found a tortousity factor of about 1,25 for both positive and negative leaders, thus slightly lower than found by Tanaka et al.

Table 1. The empirical coefficients α and β for the interpolation equations (6)-(9).

Current	α_E	β_E	α_L	β_L	α_R	β_R
100 A	506	0,139	1,16	0,266	0,169	0,295
500 A	317	0,210	1,49	0,196	0,410	0,411
2000 A	299	0,179	1,33	0,0905	0,529	0,337

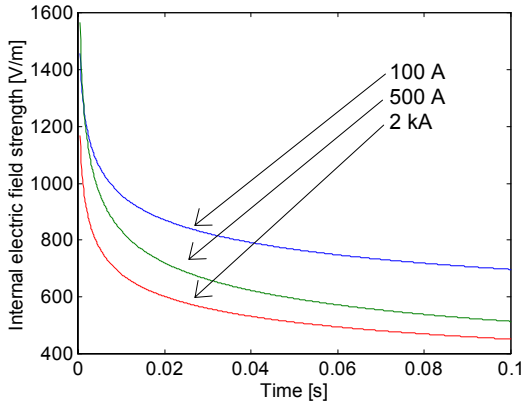

Figure 5. The development in time of the voltage gradient of the arc channel according to equation (6) for the three different arc currents.

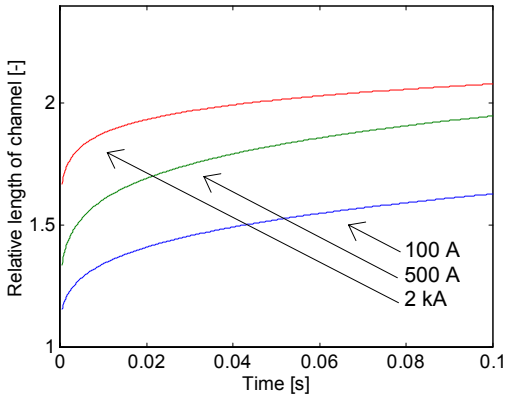

Figure 6. The development in time of the relative length of the arc channel (true arc length divided by gap distance) according to equation (7) for the three different arc currents.

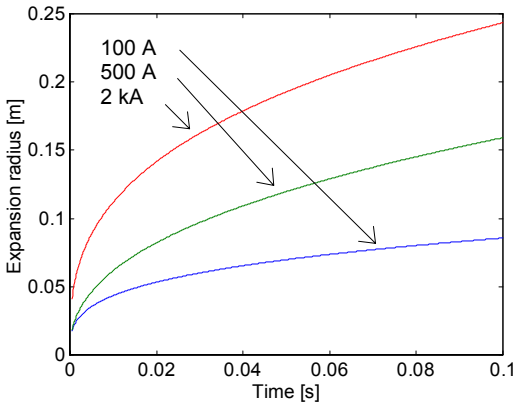

Figure 7. The development in time of the magnitude of the expansion radius according to equation (8) for the three different arc currents.

From the video recordings, they have estimated the lifting velocity, that is, the velocity of the arc channel in the vertical plane along the electrode gap. The conditions were as follows: Arc current: 0,1 - 10 kA; time duration of arc current: 0,1 - 0,2 s; gap distance: 1,3 - 3,0 m. No influence of gap distance is reported. They present the following empirical formula for the velocity as a function of the arc current:

$$v = 0{,}081 \cdot I^{0{,}71} \tag{9}$$

which is plotted in Figure 8.

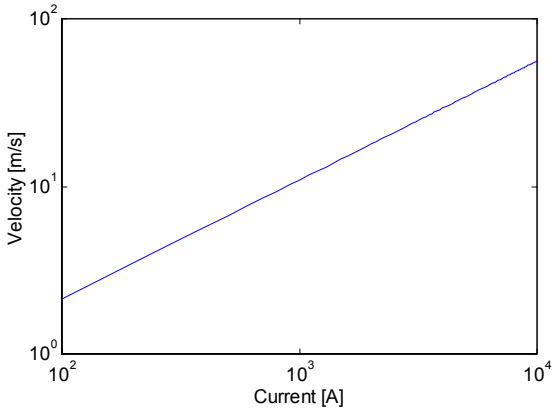

Figure 8. The vertical velocity of a horizontal arc channel as a function of the arc current according to equation (9).

6.2 Analytical expressions

Two theoretical treatments give the internal electric field strength as a function of both the current and the airflow velocity. Bublievskii studied the thermal losses of an arc channel that was balanced by aerodynamic and magnetic fields [20]. Pellerin et al studied the behaviour of a magnetically driven arc, so-called 'glidarc'[21]. They reached to the following expressions for the internal electric field

$$E_{Bub} = 1{,}83 \cdot 10^3 \left(\frac{v^2}{I} \right)^{1/3} \tag{10}$$

$$E_{Pel} = 5{,}3 \cdot 10^3 \frac{v^{0{,}48}}{I^{0{,}52}} \tag{11}$$

Both these expressions are validated against experimental data presented by the respective author. These expressions are plotted in Figure 9 for three different values of the airflow velocity (1 m/s, 5 m/s and 10 m/s).

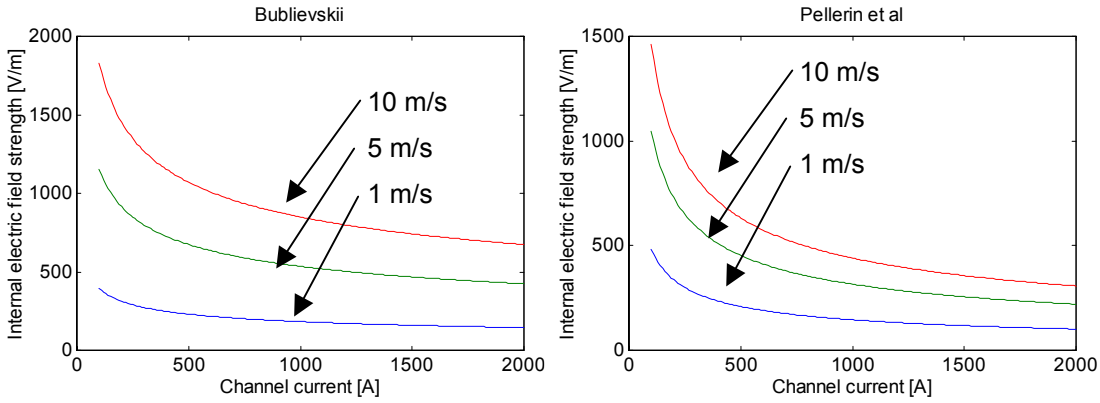

Figure 9. The internal electric field of an arc channel according to Bublievskii (left, equation (10)) and Pellerin et al (right, equation (11)).

The curves in Figure 9 appears to be consistent with the steady-state magnitudes of the voltage gradient as shown in Figure 5. If combining the Pellerin et al's expression (equation (11)) with the expression for the arc lifting velocity (equation (9)), one yields:

$$E_{Pel} = 1{,}6 \cdot 10^3 \cdot I^{-0{,}18}. \tag{12}$$

This expression is plotted in Figure 10. The figure reveals a satisfying agreement with the data inferred from Figure 5, that is, a voltage gradient of 450 – 700 V/m for current of 2000 – 100 A

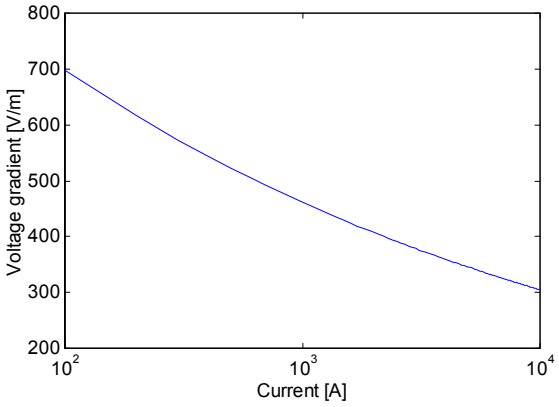

Figure 10. The internal electric field of an arc channel according to the expression by Pellerin et al combined with the Japanese expression for the velocity of the arc movement (equation (12)).

6.3 Summing up

To conclude. The recommendation is to use equation (12) for the voltage gradient along the lightning channel during the continuing current phase corrected with the tortuous path of the channel as shown in Figure 6. The tortuosity factor is about 2. Thus, the axial voltage gradient of the lightning channel for the continuous current phase is given by:

$$E_{\text{cont}} = 3 \cdot 10^3 \cdot I^{-0,18}. \tag{13}$$

To include corrections for atmospheric conditions, this expression must be normalised to standard atmospheric conditions (p_0 = 1013 hPa, T_0 = 293 K), that is

$$E_{\text{cont}} = 3 \cdot 10^3 \cdot \eta \cdot I^{-0,18}. \tag{14}$$

where η is

$$\eta = \frac{p}{p_0}\frac{T_0}{T}. \tag{15}$$

where p and T are the ambient pressure and temperature, respectively.

7. Conclusions

The following conclusions can be made

- During return stokes and recoil leaders, the inductive part of the voltage gradient along a lightning channel is prevailing.
- After return strokes and recoil leaders, the channel decays to a non-conducting state or to a steady state voltage gradient in a time of the order of 1 ms.
- During the continuing current phase, equation (14) gives the voltage gradient along the lightning channel.

References

[1] A Larsson, Ph Lalande, A Bondiou-Clergerie and A Delannoy, "The lightning swept stroke along an aircraft in flight. Part I: Thermodynamic and electric properties of lightning arc channels", Journal of Physics D: Applied Physics, Vol. 33, No 15, pp. 1866-1875 (2000)

[2] A Larsson, Ph Lalande and A Bondiou-Clergerie, "The lightning swept stroke along an aircraft in flight. Part II: Numerical simulations of the complete process", Journal of Physics D: Applied Physics, Vol. 33, No 15, pp. 1876-1883 (2000)

[3] A Larsson, A Bondiou-Clergerie, Ph Lalande, A Delannoy and S Dupraz, "New methodology for determining the extension of lightning swept stroke zones on airborne vehicles", *selected for publication in* SAE 2001 Transactions – Journal of Aerospace, 2002 (*also at* Int'l Conf on Lightning and Static Electricity (ICOLSE), Seattle, USA, 2001)

[4] A Larsson and P Lalande, "The voltage gradient along a lightning channel during strikes to aircraft", Int'l Conf on Atmospheric Electricity, Versailles, France, 9-13 June 2003 (*abstract submitted*)

[5] A Larsson, "Physical processes during lightning strike to aircraft", Compte Rendus Physique (*accepted, scheduled for december 2002*).

[6] P Lalande, A Bondiou-Clergerie and P Laroche, "Analysis of available in-flight measurements of lightning strikes to aircraft", Int. Conf. on Lightning and Static Electricity, Toulouse, France (1999)

[7] V Mazur, "Physical processes during development of lightning flashes", C R Physique, *this issue* (2002)

[8] IEC 61312-1, *Protection against lightning electromagnetic impulse - Part 1: General principles* (1995)

[9] R Thottappillil, "Electromagnetic pulse environment of cloud-to-ground lightning for EMC studies", IEEE Trans on Electromagnetic Compatibility, Vol 44, pp 203-213 (2002)

[10] E Bazelyan and Yu Raizer, *Lightning Physics and Lightning Protection*, Bristol: Institute of Physics Publishing (2000)

[11] I Gallimberti and S Stangherlin, “Thermodynamic decay of the leader channel after the discharge arrest”, IEE Proc-A, Vol 133, pp 431-437 (1986)

[12] J J Lowke, R E Voshall and H C Ludwig, “Decay of electrical conductance and temperature of arc plasmas”, J Appl Phys, Vol 44, pp 3513-3523 (1973)

[13] N L Aleksandrov, E M Bazelyan and M N Shneider, "Effect of continuous current during pauses between successive strokes on the decay of the lightning channel", Plasma Physics Reports, Vol 26, pp 952-960 (2000)

[14] K Sunabe and T Inaba, "Electric and moving characteristics of DC kiloampere high-current arcs in atmospheric air", Electrical Engineering in Japan, Vol 110, pp 9-20 (1990)

[15] S Tanaka, K Sunabe and Y Goda, "Three dimensional analysis of DC free arc behavior by image processing technique – Construction of estimation method of column path and analysis of long gap horizontal free arc behaviour", Yokosuka Research Laboratory Rep. No. W98008, Central Research Institute of Electric Power Industry (in Japanese)

[16] S Tanaka, K Sunabe and Y Goda, "Three dimensional analysis of DC free arc behavior by image processing technique (part 2) – Characteristics of voltage gradient and behavior of arc column in long gap arc", Yokosuka Research Laboratory Rep. No. W99023, Central Research Institute of Electric Power Industry (in Japanese)

[17] S Tanaka, K Sunabe and Y Goda, “Three dimensional behaviour analysis of DC free arc column by image processing technique”, XIII Int’l Conf on Gas Discharges and their Applications, Glasgow, UK, Paper No A41 (2000)

[18] Les Renardières Group, ”Positive discharges in long air gaps at Les Renardières -1975 results and discussion-”, Electra No 53, pp 32-153 (1977), p. 138

[19] Les Renardières Group, ”Negative discharges in long air gaps at Les Renardières -1978 results-”, Electra No 74, pp 67-218 (1977), p. 100

[20] A F Bublievskii, “An approximative model of an electric arc in transverse mutually perpendicular aerodynamic and magnetic fields” Journal of Engineering Physics, Vol 35, pp 1424-1429 (1978)

[21] S Pellerin, F Richard, J Chapelle, J-M Cormier and K Musiol, “Heat string model of bi-dimensional DC glidarc”, Journal of Physics D: Applied Physics, Vol 33, pp 2407-2419 (2000)